Full Characterization of a Three-Photon Greenberger-Horne-Zeilinger State Using Quantum State Tomography

K. J. Resch,[1,*] P. Walther,[1,*] and A. Zeilinger[1,2]

[1]Institut für Experimentalphysik, Universität Wien, Boltzmanngasse 5, 1090 Vienna, Austria
[2]Institut für Quantenoptik und Quanteninformation, Österreichische Akademie der Wissenschaften, Austria
(Received 1 July 2004; published 24 February 2005)

We have performed the first experimental tomographic reconstruction of a three-photon polarization state. Quantum state tomography is a powerful tool for fully describing the density matrix of a quantum system. We measured 64 three-photon polarization correlations and used a ''maximum-likelihood'' reconstruction method to reconstruct the Greenberger-Horne-Zeilinger state. The entanglement class has been characterized using an entanglement witness operator and the maximum predicted values for the Mermin inequality were extracted.

DOI: 10.1103/PhysRevLett.94.070402 PACS numbers: 03.65.Ud, 03.65.Wj, 03.67.Mn, 42.50.Xa

As quantum information processing becomes more powerful, more powerful ways of characterizing quantum states, their properties, and quantum logic operations acting upon them become necessary. States are characterized using quantum state tomography; in this technique, projective measurements are performed on an ensemble of identically prepared quantum states each probing the state from a different ''perspective''. The results of these different measurements are then used to reconstruct the complete object—the density matrix of the quantum state. Quantum state tomography techniques have characterized two-photon polarization states with varying amounts of mixedness and entanglement [1,2], orbital angular momentum states [3], Wigner functions of nonclassical states of light [4], trapped ions [5], NMR [6], and atomic states in optical lattices [7].

It is an experimental challenge to perform tomography on multiphoton states for two main reasons. Firstly, the number of measurements grows exponentially with the number of photons; the reconstruction of the polarization state of n photons necessitates $2^{2n} - 1$ n-fold coincidence measurements plus one more for normalization. In addition, three-photon and four-photon sources relying on two independent down-conversion pairs are orders of magnitude dimmer than two-photon sources. Recently, work has been reported on multiphoton triggered two-photon tomography for measuring subsystems of W states [8] and for entanglement purification [9]. In this Letter, we describe the first experiment in which the polarization state of three photons, specifically a Greenberger-Horne-Zeilinger (GHZ) state [10,11], has been completely reconstructed via quantum state tomography.

The polarization state of three photons is described by an 8×8 density matrix. To reconstruct this matrix requires a set of 64 linearly independent threefold coincidence measurements on a large ensemble of identically prepared quantum states. We use the 64 combinations of polarization measurements $|H\rangle$, $|V\rangle$, $|D\rangle = 1/\sqrt{2}(|H\rangle + |V\rangle)$, $|R\rangle = 1/\sqrt{2}(|H\rangle - i|V\rangle)$ on each photon in the three-photon coincidence subspace. Each measurement corresponds to a projection onto a pure state $|\psi_v\rangle$. The number of successful measurement outcomes is directly proportional to the expectation value $\langle\psi_v|\rho|\psi_v\rangle$ with a constant of proportionality given by the state flux $\mathcal{N}$. The density matrix is reconstructed by an inversion algorithm. Because of experimental imperfections, linear inversion can lead to unphysical density matrices making calculation of certain important properties (e.g., the concurrence [12]) impossible. These problems can be avoided using a maximum-likelihood reconstruction [13]. We employ the specific method of James *et al.* [14]. Uncertainties in quantities extracted from these density matrices were calculated using a Monte Carlo routine and assumed Poissonian errors.

Our experimental setup is shown in Fig. 1. The second harmonic of a modelocked Ti:Sapphire laser passes twice through a 2 mm long, type-II phase-matched β-barium borate (BBO) crystal and creates polarization-entangled photon pairs [15]. The transverse and longitudinal walk-off effects are compensated by additional half-wave plates (HWP) and extra BBO crystals (COMP). By rotating the polarization with an additional HWP, one for each pair, and tilting the compensation crystals, any of the four Bell states can be produced. We align the source such that the Bell states $|\phi^+\rangle = 1/\sqrt{2}(|HH\rangle + |VV\rangle)$ are created on each pass of the pump. After the optical elements, including 3 nm bandwidth filters, the light is coupled into single-mode fibers which direct the light to fiber-coupled single-photon counting detectors. Experimentally measured two-fold coincidence rates were 27 000 s^{-1} (19 000 s^{-1}) for the forward-emitted (backward-emitted) pairs.

When the source creates two pairs of entangled photons in the desired modes, our initial state is described by $|\Psi\rangle_{1234} = |\phi^+\rangle_{12} \otimes |\phi^+\rangle_{34}$, where subscripts label the spatial modes. GHZ entanglement is created using a polarizing beam-splitter (PBS). The PBS is a linear optical

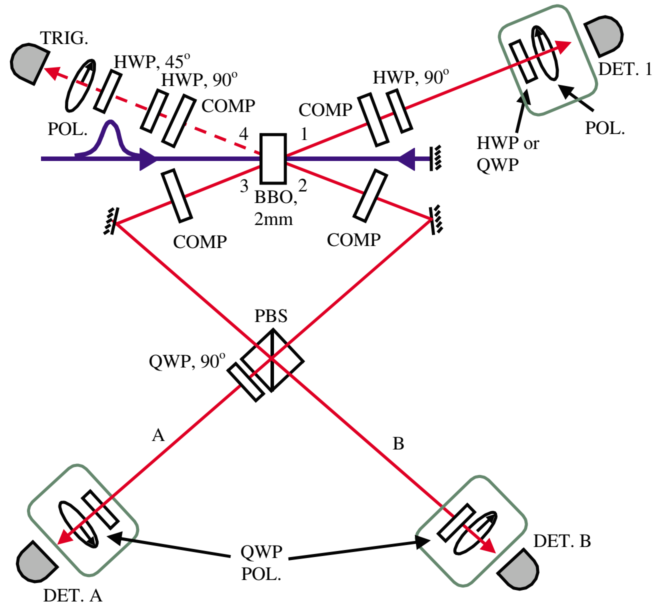

FIG. 1 (color online). Experimental Setup. An ultraviolet laser pulse makes two passes through a type-II phase-matched BBO crystal. This probabilistically produces two pairs of photons into the four modes (1-4). A HWP and compensation crystal (COMP) are placed in each path to counter walk-off effects. The polarization of one photon from each pair are rotated by 90° using HWPs to create a pair of $|\phi^+\rangle$ states. These two independent photon pairs are further entangled using the PBS provided that the photons in mode 2 and 3 overlap temporally. The three-photon GHZ state was produced between modes A, B, and 1 when photon 4 is successfully projected onto the state $|D\rangle_4$ signalled by a click at the trigger detector (TRIG.). Tomographic projections were performed using QWPs and polarizers (POL.) for photons at detectors A and B and a half-wave or quarter-wave plate in front of a fixed horizontal polarizer at detector 1. An additional quarter-wave plate was used in mode A to cancel an unwanted phase shift from the PBS.

element that transmits horizontally polarized light and reflects vertically polarized light. In conjunction with post-selection of those cases where incident photons in modes 2 and 3 emerge from different output ports A and B, the PBS acts as a quantum parity check [16]—the photons must have had the same polarization in the H/V basis. When photons in modes 2 and 3 arrive at the PBS simultaneously within their coherence lengths and we keep only those cases where the photons emerge into different output ports, our state is conditionally transformed as: $1/2(|HH\rangle_{12} + |VV\rangle_{12}) \otimes (|HH\rangle_{34} + |VV\rangle_{34}) \rightarrow 1/\sqrt{2}(|HHHH\rangle_{AB14} + |VVVV\rangle_{AB14})$ [17]. This four-photon GHZ state is reduced to the three-photon GHZ state $|\mathrm{GHZ}\rangle = 1/\sqrt{2}(|HHH\rangle_{AB1} + |VVV\rangle_{AB1})$ upon successful projection of the photon in mode 4 onto the polarization state $|D\rangle_4$.

We perform tomographic measurements using wave plates and polarizers. In modes A and B, quarter-wave plates (QWPs) and freely rotatable polarizers are used to make projections onto the polarizations $\{H, V, D, R\}$. In the actual experiment, modes 1 and 4 were folded over one another and crossed at a second PBS followed by two horizontal polarizers. In this configuration, only transmitted photons can be detected and this PBS-polarizer combination acts as a pair of fixed horizontal polarizers. Since the polarizer in mode 1 could not be rotated, we required both quarter-wave and half-wave plates to make our projections. A fourfold coincidence between the single-photon counting detectors in modes A, B, 1, and 4 signals the following: (1) the creation of two pairs of photons, (2) the multiphoton entangling operation of the PBS and creation of the four-photon GHZ state (3) the projection onto $|D\rangle_4$ to create our three-photon GHZ state, and (4) a successful outcome for our tomographic measurement.

In order to demonstrate that our photons were entangled, we measured modes 1 and 4 in the polarization state $|D\rangle$. For the desired GHZ state, this leaves the photons in modes A and B in the Bell state $|\phi^+\rangle_{AB}$. Recall $|\phi^+\rangle = 1/\sqrt{2}(|HH\rangle + |VV\rangle) = 1/\sqrt{2}(|DD\rangle + |AA\rangle)$, where $|A\rangle = 1/\sqrt{2}(|H\rangle - |V\rangle)$; i.e., its polarizations are not only perfectly correlated in the H/V basis but also in the D/A basis. However, if the photons in modes 2 and 3 do not overlap at the PBS, then the two paths leading to a

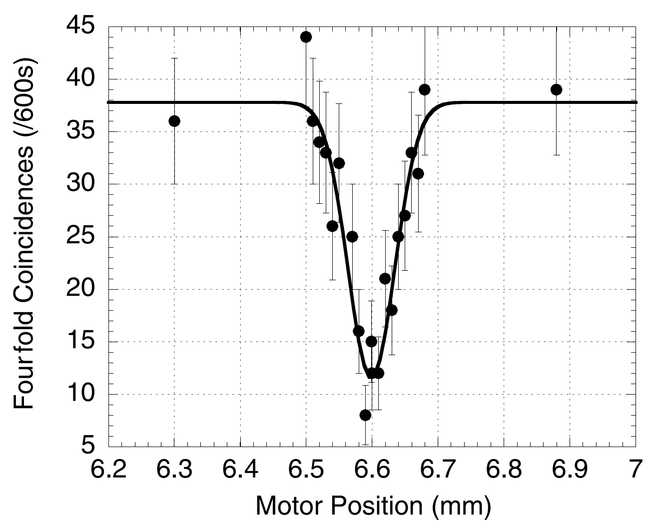

FIG. 2. Fourfold coincidences versus pump mirror position. The source produces two pairs of photons in the state $|\phi^+\rangle$—one pair into modes 1 and 2 and the other into modes 3 and 4. For this measurement, the photons in modes 1 and 4 were successfully projected onto the state $|D\rangle$. As the pump mirror is displaced, the overlap between the photons in modes 2 and 3 is changed. If the photons do not overlap, then the outputs of PBS have no correlations in the D/A-basis. However, if the photons overlap perfectly, then the outputs of the PBS are left in the state $|\phi^+\rangle$ which has strong correlations. The changes in the correlations manifest as an interference dip when the output modes A and B of the PBS are measured in the states $|A\rangle$ and $|D\rangle$. The visibility of the dip is $(69 \pm 5)\%$.

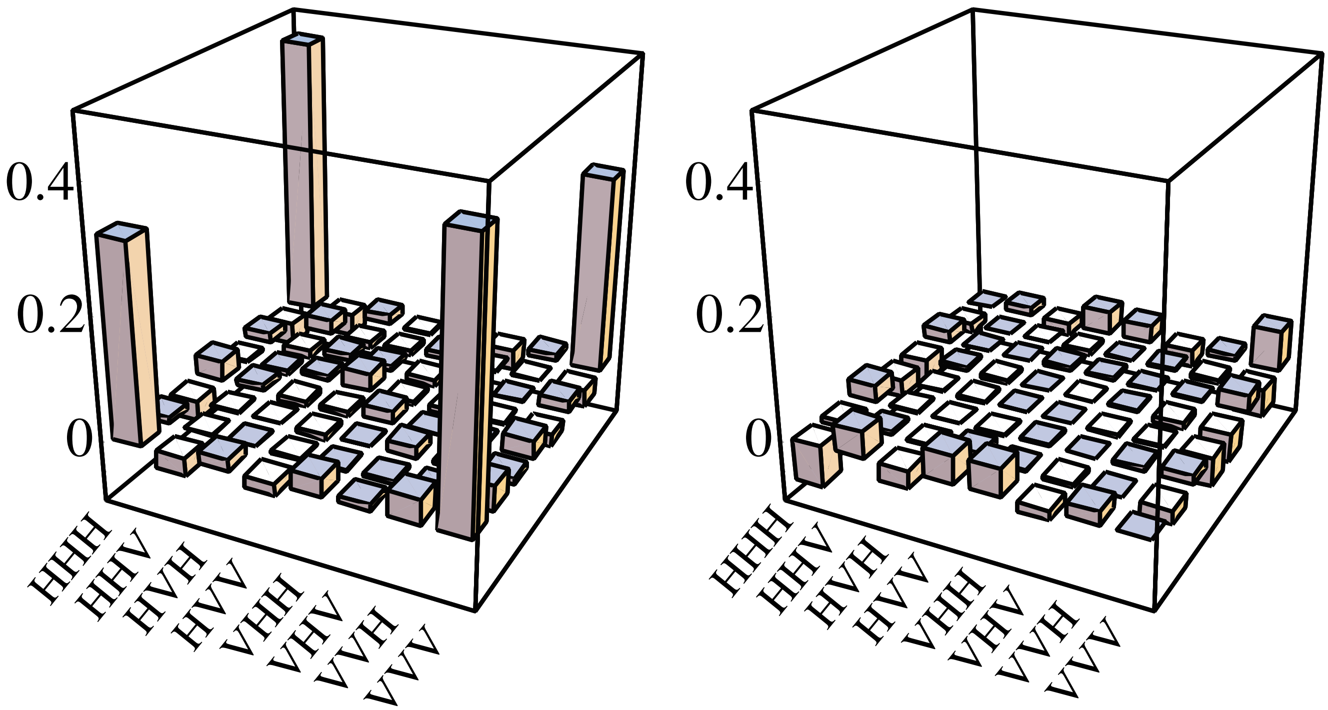

FIG. 3 (color). Density matrix of a three-photon GHZ state. The real (left hand) and imaginary (right hand) of the density matrix were reconstructed from 64 linearly independent triggered threefold coincidence measurements. Large diagonal elements in the $|HHH\rangle$ and $|VVV\rangle$ positions along with large positive coherences indicate that this state has the qualities of the desired GHZ state. Those elements that have negative values are shown as white-topped bars while those that are positive are blue topped.

photon in each of modes A and B are distinguishable. This leaves the photons instead in the half-mixed state $\rho = 1/2(|HH\rangle\langle HH| + |VV\rangle\langle VV|)$. The correlations of this state are identical to $|\phi^+\rangle$ in the H/V basis, but it has no correlations in the D/A basis. With the polarizers in modes A and B set to $|A\rangle$ and $|D\rangle$ respectively, we record four-photon coincidences as a function of the delay mirror position. The results are shown in Fig. 2 and demonstrate the change in the correlations when the photons from the independent pairs arrive at the PBS simultaneously. The correlation change is observable as a $(69 \pm 5)\%$ visibility dip in the fourfold rate. Tomographic measurements were all taken at the center of this interference dip where the interference is a result of the requisite coherent superposition. Note that a QWP was placed in output mode A at 90° to compensate birefringence in the PBS. Each tomographic measurement took 900 s and yielded a maximum 466 fourfold counts for the $|VVV\rangle$ projection. To account for laser fluctuations over this time, we normalized our data by dividing by the square of the background-corrected singles at the trigger detector (detector 4). The leading-order background in our fourfold coincidence signal comes from accidental twofold coincidence counts at the same time as real two folds. These rates were estimated from measured singles and twofold coincidence data and subtracted from our signal.

The three-photon density matrix reconstructed from the entire data set of 64 measurements is shown in Fig. 3. On the diagonal of the matrix, the dominant elements are those corresponding to $|HHH\rangle$ and $|VVV\rangle$. Furthermore, there are strong and mostly positive coherences between these elements with a small phase shift appearing in the imaginary part. Thus our state has the qualitative properties of the GHZ state. The fidelity of our state with the ideal GHZ state, $\mathcal{F}_{\rm GHZ} = \langle {\rm GHZ}|\rho|{\rm GHZ}\rangle = (76.8 \pm 1.5)\%$ provides quantitative confirmation. Entanglement measures for pure and mixed 2-qubit states are well-known, but the same is not true for 3-qubit states. With two qubits, the states are either separable or entangled, however with three qubits there exist two nonequivalent classes of 3-qubit entanglement called GHZ and W [18]. We characterize our state using an entanglement witness operator which detects GHZ entanglement, $\mathcal{W} = 3/4I - P_{\rm GHZ}$, where I is the identity and $P_{\rm GHZ}$ is a projector onto a GHZ state [19,20]. When the expectation value of this witness operator, ${\rm Tr}\mathcal{W}\rho$, is negative, the state definitely contains GHZ entanglement. The minimum expectation value for this witness operator and our density matrix for those states related to $|{\rm GHZ}\rangle$ by local, single-qubit, unitary transformations is $\langle\mathcal{W}\rangle_{\rm MIN} = -0.044 \pm 0.016$, which is negative by almost 3 standard deviations.

Fully reconstructed density matrices are a complete description of the quantum state and can be used to predict the outcomes of any other measurements one could have performed. As an explicit example of the usefulness of such an approach, we will investigate what nonlocal properties our state could exhibit in a Bell experiment. The classic Clauser-Horne-Shimony-Holt (CHSH)-Bell inequalities are not directly applicable to 3-qubit states [21]. An inequality based on the assumptions of local realism was derived by Mermin [22] and can be stated using the expression $M = |E(ABC') + E(AB'C) + E(A'BC) - E(A'B'C')|$, where A and A', B and B', and C and C' can be different polarization measurement settings made on photons A, B, and 1, respectively, and E is the expectation value of the polarization correlation for those settings [23]. Any local realistic theory places a strict limit on the maximum strength of measured correlations such that $M \leq 2$. Our density matrix *predicts* the maximum possible Mermin parameter $M_{\mathrm{MAX}} = 2.73 \pm 0.11$. Thus our state is able to violate the Mermin inequality and show a violation of local realism by 6.6 standard deviations.

In this experiment, we have created a three-photon GHZ state, performed a tomographically complete set of polarization measurements, and reconstructed its density matrix. The most important consequence of reconstructing the complete density matrix of a quantum state is that one can use this reconstruction to find out whether the state fulfills criteria in any possible experiment. Using an entanglement witness we have shown that our state lies within the GHZ class of 3-qubit entangled states. Our state is able to demonstrate a conflict with local realism through a Mermin inequality. This work is a significant step towards measuring and understanding real multiparticle entangled states.

We thank A. Steinberg and M. Mitchell for computer software and Č. Brukner, C. Ellenor, K. Hornberger, A. Stefanov, A. Steinberg, A. White, and M. Żukowski for helpful discussions. This work was supported by ARC Seibersdorf Research GmbH, the Austrian Science Foundation (FWF), project no. SFB 015 P06, NSERC, and the European Commission, contract no. IST-2001-38864 (RAMBOQ).

*Corresponding author.

[1] A. G. White *et al.*, Phys. Rev. Lett. **83**, 3103 (1999); A. G. White *et al.*, Phys. Rev. A **65**, 012301 (2002).
[2] N. A. Peters *et al.*, Phys. Rev. Lett. **92**, 133601 (2004).
[3] G. Molina-Terriza *et al.*, Phys. Rev. Lett. **92**, 167903 (2004); N. K. Langford *et al.*, Phys. Rev. Lett. **93**, 053601 (2004).
[4] D. T. Smithey *et al.*, Phys. Rev. Lett. **70**, 1244 (1993); A. I. Lvovsky *et al.*, Phys. Rev. Lett., **87** 050402 (2001).
[5] C. F. Roos *et al.*, Phys. Rev. Lett. **92**, 220402 (2004).
[6] I. L. Chuang *et al.*, Proc. R. Soc. London A **454**, 447 (1998).
[7] S. H. Myrskog *et al.*, quant-ph/0312210.
[8] M. Eibl *et al.*, Phys. Rev. Lett. **92**, 077901 (2004).
[9] P. Walther *et al.*, Phys. Rev. Lett. **94**, 040504 (2005).
[10] D. M. Greenberger, M. A. Horne, and A. Zeilinger, in *Bell's Theorem, Quantum Theory, and Conceptions of the Universe*, edited by M. Kafatos (Kluwer Academics, Dordrecht, The Netherlands 1989), p. 73.
[11] D. Bouwmeester *et al.*, Phys. Rev. Lett. **82**, 1345 (1999); J.-W. Pan *et al.*, Nature (London) **403**, 515 (2000).
[12] W. K. Wootters, Phys. Rev. Lett. **80**, 2245 (1998); V. Coffman, J. Kundu, and W. K. Wootters, Phys. Rev. A **61**, 052306 (2000).
[13] Z. Hradil, Phys. Rev. A **55**, R1561 (1997); K. Banaszek *et al.*, Phys. Rev. A **61**, 010304(R) (1999).
[14] D. F. V. James *et al.*, Phys. Rev. A **64**, 052312 (2001).
[15] P. G. Kwiat *et al.*, Phys. Rev. Lett.,**75**, 4337 (1995).
[16] T. B. Pittman, B. C. Jacobs, and J. D. Franson, Phys. Rev. A **64**, 062311 (2001); J.-W. Pan *et al.*, Nature (London) **410**, 1067 (2001); J.-W. Pan *et al.*, *ibid.* **423**, 417 (2003).
[17] Z. Zhao *et al.*, Phys. Rev. Lett. **91**, 180401 (2003).
[18] W. Dür, G. Vidal, and J. I. Cirac, Phys. Rev. A **62**, 062314 (2000).
[19] M. Horodecki, P. Horodecki, and R. Horodecki, Phys. Lett. A, **223**, 1 (1996); B. H. Terhal, Phys. Lett. A **271**, 319 (2000); M. Lewenstein *et al.*, Phys. Rev. A **62**, 052310 (2000); M. Bourennane *et al.*, Phys. Rev. Lett. **92**, 087902 (2004).
[20] A. Acín *et al.*, Phys. Rev. Lett. **87**, 040401 (2001).
[21] J. Bell, Physics (Long Island City, N.Y.) **1**, 195 (1964); J. F. Clauser, M. A. Horne, A. Shimony, and R. Holt, Phys. Rev. Lett. **23**, 880 (1969).
[22] N. D. Mermin, Phys. Rev. Lett. **65**, 1838 (1990).
[23] J. L. Cereceda, Phys. Rev. A **66**, 024102 (2002).